Ex vivo analysis of local orientation of collagen fiber bundles in 3D in posterior horn human meniscus using micro-computed tomography

Ville-Pauli Karjalainen

Master's Thesis

Medical and Wellness Technology

Faculty of Medicine

University of Oulu

2021

Karjalainen Ville-Pauli (2021), Ex vivo analysis of local orientation of collagen fiber bundles in 3D in posterior horn human meniscus using micro-computed tomography, Faculty of Medicine, University of Oulu, Master's Thesis, 36+21 Pages

Abstract

Objective: Knee osteoarthritis (OA) is an increasingly relevant joint disease affecting mostly aged population in developed countries. However, there is currently no treatment for OA and increasing the knowledge of the disease with the help of micro-computed tomography (μCT) imaging could offer help in finding the solution. The objective of this thesis was to quantitatively analyze the microstructural organization of human posterior horn meniscus samples in 3D using hexamethyldisilazane (HMDS) based μCT imaging. In addition, this study aims to compare the local microstructural organization of meniscus between OA patients and healthy references.

Method: We collected medial and lateral posterior horns of human menisci from 10 end-stage medial compartment knee OA patients undergoing total knee replacement surgery and from 10 deceased donors without diagnosed knee OA to act as healthy reference. The posterior horns were dissected and fixed in formalin, dehydrated in ascending alcohol concentrations, treated with HMDS, and scanned with a desktop μCT. Furthermore, we performed local orientation analysis of collagenous microstructure in 3D to all samples, by calculating local structure tensors from greyscale gradients withing a selected integration window to determine the polar angle for each voxel. Moreover, distribution of angles and mean estimated average angles were statistically compared.

Results: Collagen fiber bundles in HMDS-treated meniscal samples were depicted in 3D using μCT. In the quantitative local orientation analysis, medial OA had overall lowest orientation angles compared to all other groups: mean estimated differences versus medial OA were -24° [95%CI -31°, -18°] in medial donor, -25° [95%CI -34°, -15°] in lateral OA, and -25° [95%CI -35°, -16°] in lateral donor groups. Distribution and mean angles between lateral OA and lateral donor menisci were similar with a mean difference of 2°.

Conclusions: In this study, we were able to quantitatively analyze collagen fiber bundles and their orientations in 3D in the posterior horn of human meniscus using HMDS-based

μCT imaging. Furthermore, collagen disorganization increased in the medial OA meniscus, suggesting a relationship between collagenous microstructure disorganization and meniscus degradation.

Keywords: Osteoarthritis, micro-computed tomography, meniscus, collagen, local orientation, hexamethyldisilazane

Karjalainen Ville-Pauli (2021), Ihmisen nivelkierukan takasarven kollageenisäiekimppujen kolmiulotteinen lokaaliorientaatioanalyysi mikrotietokonetomografian avulla**, Lääketieteellinen tiedekunta, Oulun yliopisto, Pro gradu - tutkielma, 36+21 sivua**

Tiivistelmä

Tarkoitus: Nivelrikko on yleinen sairaus vanhenevassa yhteiskunnassa, mutta sairauden monimuotoisuuden vuoksi sen hoitaminen on vaikeaa. Sairauden vahvempi ymmärtäminen voisi auttaa hoidon kehittämisessä sairautta vastaan. Tämän pro gradu -tutkielman tavoitteena oli analysoida kvantitatiivisesti ihmisen nivelkierukkanäytteiden mikrorakenteiden orientaatiota kolmiulotteisesti käyttäen heksametyylidisilatsaaniin (HMDS) perustuvaa näytteenkäsittelytekniikkaa mikrotietokonetomografiakuvantamisessa (μCT). Lisäksi tässä työssä verrataan kierukan lokaalimikrorakenneorganisaatiota nivelrikkoisten potilaiden ja terveiden verrokkien välillä.

Menetelmä: Keräsimme mediaali- ja lateraalipuolen nivelkierukan takasarvet kymmeneltä nivelrikon loppuvaiheen potilaalta, joille tehtiin polven tekonivelleikkaus, ja 10 menehtyneeltä oikeuslääketieteen potilaalta, joilla ei ollut diagnosoitua polven nivelrikkoa. Nivelkierukoiden posterioriset sarvet leikattiin, käsiteltiin formaliinilla, kuivattiin nousevissa etanolipitoisuuksissa, käsiteltiin HMDS:llä ja kuvattiin μCT-laitteella. Lisäksi teimme näytteille kolmiulotteisen orientaatioanalyysin, jolla mitataan näytteiden kollageenisen mikrorakenteen orientaatiota. Analyysi laskee μCT-kuvien harmaasävygradienttien avulla jokaiselle vokselille paikallisen rakennetensorin, joiden purkamisesta saadaan laskettua vokselin anisotropian määrä ja sen pienimmän vektorin suunta. Pienin arvo ja sen suunta voidaan määrittää vokselin pääasialliseksi orientaatioksi. Kulmien jakautumista ja keskimääräisiä kulmia verrattiin tilastollisesti terveiden ja nivelrikkopotilaiden mediaali- ja lateraalipuolten välillä.

Tulokset: Nivelkierukan kollageenikimput kuvattiin kolmiulotteisesti μCT:llä käyttäen HMDS-käsiteltyjä nivelkierukkanäytteitä. Kvantitatiivisessa orientaatioanalyysissä todettiin mediaalipuolen nivelrikkoisilla nivelkierukoilla yleisesti enemmän disorganisaatiota kaikkiin muihin ryhmiin verrattuna: mediaalipuolen nivelrikkoryhmässä orientaatioiden ero verrattuna mediaaliverrokkiryhmään oli -24° [95%CI -31°, -18°], -25° [95%CI -34°, -15°] verrattuna lateraalipuolen nivelrikkoryhmään ja -25° [95%CI -35°, -16°] ver-

rattuna lateraalipuolen luovuttajaryhmän välillä. Lisäksi lateraalipuolen luovuttaja- ja lateraalipuolen nivelrikkoryhmän välillä kulmien jakauma ja keskiarvo olivat samanlaiset keskimäärisen eron ollessa 2°.

Johtopäätökset: Tässä tutkimuksessa onnistuimme kuvaamaan ihmisen nivelkierukan kollageenikimput sekä kvantitatiivisesti analysoimaan niiden kolmiulotteista orientaatiota käyttäen HMDS-pohjaista μCT-kuvantamista. Lisäksi kollageenin disorganisaatio oli suurin mediaalipuolen nivelrikkoisessa nivelkierukassa, mikä viittaa kollageenisen mikrorakenteen disorganisaatioon ja nivelkierukan degeneraation väliseen vahvaan suhteeseen.

Avainsanat: Nivelrikko, mikrotietokonetomografia, nivelkierukka, kollageeni, paikallisorientaatio, heksametyylidisilatsaani

FOREWORD

The study was done in the Research Unit of Medical Imaging, Physics and Technology in the University of Oulu. In this study, we wanted to analyze the microstructural collagen organization of human meniscus. The study was made possible with our state-of-the-art μCT desktop device and fascinating human meniscus samples we received from Lund, Sweden.

I would like to thank my thesis supervisors Dr. Mikko Finnilä and M.H.Sc. Iida Kestilä for their support, guidance, and patience with this thesis. I would also like to thank Prof. Simo Saarakkala for the memorable times in the research group. Thanks to our collaborators in Lund, Sweden for extracting and sending us the menisci samples and for the help with the manuscript. Finally, I would like to thank all of DIOS research group for their enthusiasm and friendship.

Oulu, 22.02.2021

Ville Karjalainen

Ville-Pauli Karjalainen

LIST OF SYMBOLS AND ABBREVIATIONS

μCT	micro-computed tomography
3D	three-dimensional
AC	articular cartilage
CEμCT	contrast-enhanced micro-computed tomography
CT	computed tomography
ECM	extracellular matrix
GAGs	glycosaminoglycans
HMDS	hexamethyldisilazane
MIL	mean intercept length
OA	osteoarthritis
PG	proteoglycan
PLM	polarized light microscopy
VO	volume orientation
VOI	volume of interest

CONTENTS

1. INTRODUCTION

Osteoarthritis (OA) is a common joint disease in elderly and it causes pain, aching, inflammation, and stiffness in the joint, limiting the movement of the whole joint[1]–[4]. Knee joint is one of the most common joints to develop OA due to its' complex biomechanics involving most of the weight-bearing of human body, anatomy and susceptibility to joint injuries[5], [6]. Thus, the whole knee joint including the tibia and femur bones and menisci are affected by OA[1]–[3].

As a complex musculoskeletal disease that affects all the compartments in the joint, OA pathology is not well understood. This complexity makes the diagnosis, treatment, and pharmacological drug development difficult. While medications may help to slow down the progression of OA and reduce inflammatory effects, no proven treatment or cure for knee OA has been developed[7]. Studying the disease further requires a closer look into the different compartments of the knee, including the meniscus.

Residing between the tibial and femoral bones within the knee joint, the menisci are wedge-shaped fibrocartilaginous tissues primarily composed of a collagenous fiber network[8]–[10]. As the menisci bear an important role in a functioning healthy knee, studying the meniscus is important for the OA research [11], [12]. The most crucial functions of meniscus is load transmission within the knee and secondary roles include shock absorption, joint stabilization, lubrication and nutrient distribution[8], [9], [13], [14].

Having multiple important functions within the knee joint, the menisci are susceptible to degeneration and injury[15]. Meniscal injury or trauma can lead to OA in the knee joint or *vice versa,* degenerative meniscal tears may manifest without any history of trauma, caused by degenerative changes within the joint caused by OA[16]. Moreover, knee OA and cartilage degeneration are highly associated with meniscal tears and degeneration[17]–[19] with loss of meniscal function being one of the highest risk factors for knee OA[20]. Both meniscal tears and knee OA cause further degeneration in the extracellular matrix (ECM) manifesting as loss of structure and disorganization of the collagenous network. Previously, polarized light microscopy (PLM) has been used to measure this collagenous fibre network orientations in cartilage in two dimensions from thin histology

slices[21]–[23]. However, these two-dimensional methods completely lose the three-dimensional (3D) information in the analyzing process. Thus, an approach to analyze these microstructural collagen fibre orientations in 3D is preferred.

Micro-computed tomography (μCT) is a well-established, non-destructive 3D imaging technique used widely in medical research[24], [25]. However, soft tissues like meniscus have a decreased ability to attenuate x-rays, so inducing a contrast enhancing agent to the meniscus is required before the imaging[26], [27]. Contrast-enhanced micro-computed tomography (CEμCT) has been previously used successfully with hexamethyldisilazane (HMDS) -based sample preparation method for *ex vivo* imaging of human AC and human posterior horn of meniscus [28], [29]. Furthermore, 3D μCT images and application of structural tensors have been used to determine ECM orientation in AC[28].

This study aims to establish a method to quantitatively analyze the microstructural organization of human meniscus *ex vivo* samples in 3D. This will be performed using an HMDS-based air-dried sample preparation method with μCT imaging to help the understanding of the complex disease. Furthermore, the study aims to quantitatively measure and compare the local microstructural organization with structural tensor analysis in meniscus posterior horn between medial and lateral menisci of OA patients and healthy donors.

This thesis is written as an article-based thesis and a pre-proof of the article is included in the appendix.

2. BACKGROUND

The thesis focuses on the meniscus microstructure and OA, therefore, the anatomy of meniscus, its contents, and the collagen structure are reviewed shortly. Moreover, I will go through how meniscus is affected in OA. Finally, μCT and different orientation analysis methods are presented briefly.

2.1 Meniscus

Meniscus is a wedge-shaped fibrocartilaginous tissue between the tibia and femur bones in the knee (Figure 1)[30]. The main function of the meniscus in the knee joint is load transmission[8], [15], [31]. Furthermore, meniscus has important secondary roles in joint stability, shock absorption and providing lubrication for the knee joint for frictionless movement[31]–[33].

The ECM of a healthy meniscus consists of a thick network of collagen fibers (15-25% of wet weight) working as principal structural component of the ECM with other constituents, including water (60-70% of wet weight), proteoglycans (PG) (1-2% of wet weight) and non-collagenous proteins, residing between the collagenous structure[34]–[37].

Collagens are the most abundant proteins in the whole human body and they also work as primary structural component providing the tensile strength of menisci[35]. PGs are large, negatively charged hydrophilic molecules within collagen network consisting of a core protein and glycosaminoglycan chains (GAGs). PGs are responsible for hydration for their ability to bind water in the ECM with their high fixed-charge density, providing the menisci their viscoelastic properties, and knee joint its high capacity to resist compressive loads[36], [38], [39].

The most abundant collagen in meniscus is collagen type I[34]. Moreover, collagen type I covers 90% of the collagens found in meniscus with small amounts of collagen types II, III, V and VI found in addition[34], [36]. In addition, collagens are fibrous proteins that provide the structural network for the fibrocartilage of meniscus[29], [40].

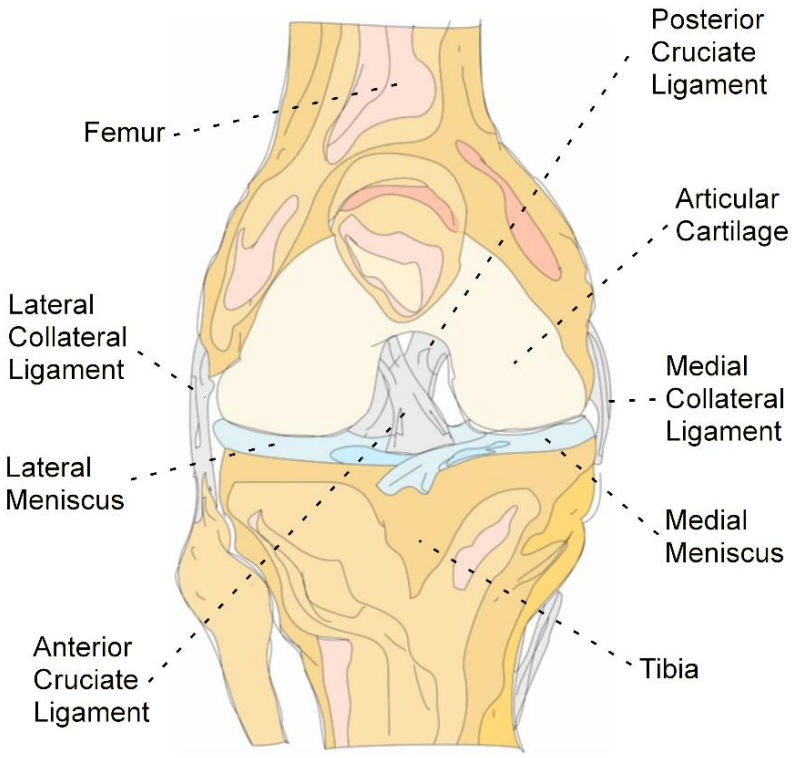

Figure 1. Front view of a right knee joint. The menisci lie between tibia and femoral bones to provide shock absorption and joint stability for the knee joint.

2.1.1 Anatomy

The menisci locate in the medial and lateral sides of the knee (Figure 2). The peripheral outer aspects of each meniscus are thick, vascularized and attached to the joint. The inner border of the meniscus is a thin free edge not attached to the joint. Both menisci are connected to the anterior and posterior cruciate ligaments from their anterior and posterior horns, respectively[30]. Posterior and anterior horns of meniscus function as attachment points between the meniscal body and subchondral bone of tibial plateaus, while the moving body transmits mechanical loads[30]. Furthermore, the menisci are connected to each other through transverse intermeniscal ligament[30].

Medial meniscus covers approximately 60% of the AC medial area with its approximate full grown diameter of 35mm in adults[39]. Moreover, while the lateral meniscus is larger and more mobile, covering 80% of the AC lateral area, the medial meniscus is more firmly attached to the knee joint through larger insertion sites for the ligaments[15], [41].

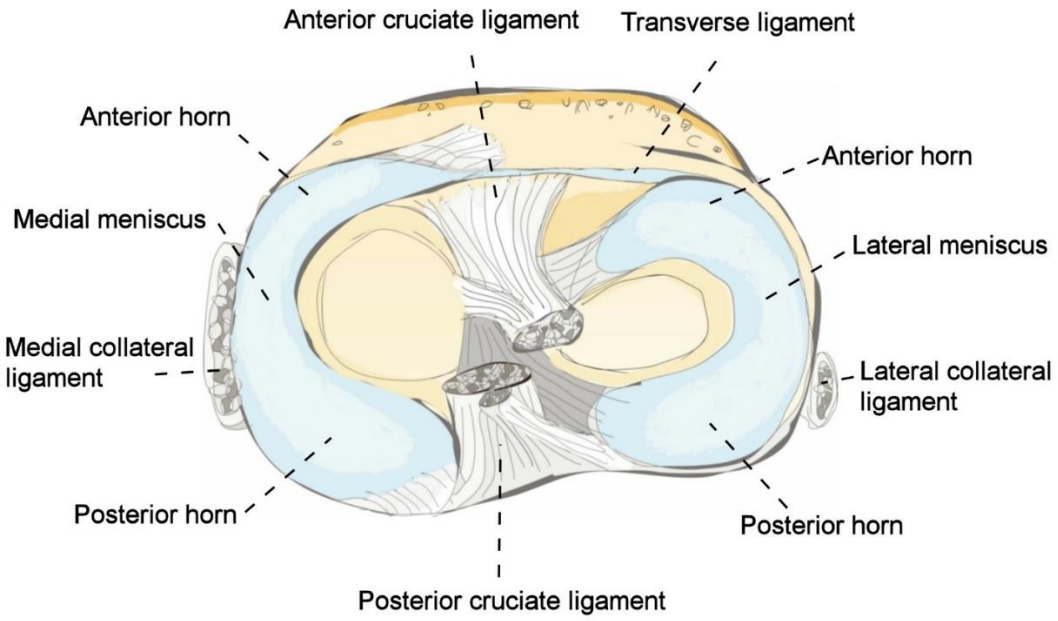

Figure 2. Anatomy of the human menisci from top down view. Both menisci are attached to the knee joint with anterior and posterior cruciate ligaments and to each other through transverse ligament.

2.1.2 Collagen organization

The collagen fibers in the meniscus are highly organized into three distinct layers, each with their own unique network as seen in Figure 3[42], [43]. Superficial layer covers both tibial and femoral surfaces of meniscus with 10µm thick collagen network of thin fibrils. In this region the collagen fibers are randomly orientated without dominant direction[43].

Lamellar layer lies beneath the superficial network forming approximately 150-200µm thick lamellae or a small plate of collagen fibrils[43]. Near the outer border of meniscus, the collagen fibers orient radially and are bound to the outer border of meniscus, as seen in Figure 3. In other parts of lamellar layer, the collagen fibers are intersecting each other at various directions, but parallel to the superficial layer, forming support structures towards the upper layer[43].

In the middle layer or central main layer, which lies between the two lamellar layers. the collagen fibers are predominantly circumferentially orientated around the inner border of meniscus[43]. However, in the middle layer region, a few radial collagen fibrils intertwine with the circumferentially oriented collagen fibrils to tie them together[30]. The thickness of middle layer is wider in the outer edge of meniscus and decreases towards the inner

edge of meniscus as seen in Figure 3. The cross-linked multilayer collagen fiber network is ideal for transferring vertical compressive load into hoop stresses from the surface of meniscus into to the circumferential middle layer[30], [32], [33].

Disruptions to the healthy collagen network such as meniscal tears or ECM degeneration weakens the biomechanical properties of meniscus[44]. Additionally, meniscal tears and degeneration of ECM are highly associated with OA[45]. Thus, preservation of the menisci's unique collagen composition and organization is crucial to a healthy knee joint[15].

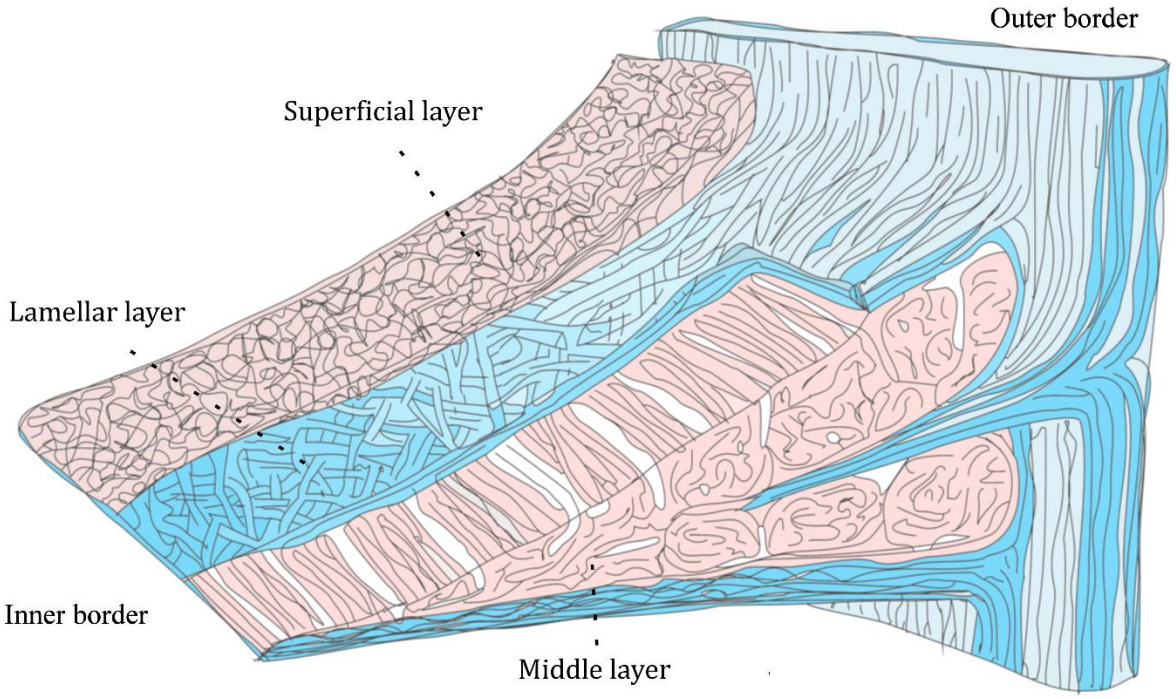

Figure 3. Meniscus is split into three distinct layers: On the surface in the superficial layer, collagen fibrils are seemingly randomly orientated in approximately 10µm thick network of fibrils covering both femoral and tibial surfaces of meniscus. The lamellar layer, a 150-200µm thick layer found below superficial layers with radially orientated fibrils extracting from the outer edge of meniscus parallel with the femoral and tibial surfaces. Middle layer; lying between the two lamellar layers, this central layer covers most of the meniscus' volume with circumferentially orientated collagen fibers. Image adapted from [43].

2.2 Osteoarthritis

OA is a complex musculoskeletal disorder and does not result from a single origin but is rather multifactorial. Thus, diagnosing the disease and treating it is extremely difficult. [46]. Moreover, the incidence of OA increases with aging population[47]. Moreover, obesity, metabolic diseases, sex, joint traumas and occupational joint stresses are all major risk factors of developing OA[1], [46], [48].

OA is the most common arthritic disease of all synovial joints causing stiffening, pain, and limitations to movement of the joint[1], [3]. Moreover, OA is not only a prominent cause of disability and morbidity, but also a formidable burden for national health institutes globally[49]. Furthermore, in 2011, hip and knee OA were ranked 11th highest contributor to disability[48]. Unfortunately, even though OA is a serious disease with increasing impact globally, there is no cure for OA available and the treatment is limited to prevention of the disease and ultimately, a hip or knee replacement surgery[1], [46].

Affecting the whole joint in the knee, OA results in a progressive wear and tear of the joint, *e.g.* causing loss of articular cartilage and thickening of underlying bone in tibia, patella and femur, but also causing degeneration of the meniscus[7], [50]. Moreover, the loss of articular cartilage and degeneration of meniscus cause the pain, aching and stiffening in the movement of the joint[3].

2.2.1 Meniscus in osteoarthritis

Meniscus' significant role in the mechanics of the knee joint make it susceptible to injuries[17]. Injury or degeneration of menisci affects the whole knee joint and greatly increases the risk of developing knee OA[17], [51]. Injuries in the meniscus usually manifest as meniscal tears, most commonly from acute knee trauma where a combination of rotational forces and axial compressive loading result in shear load[20], [52]. Thus, as a result of the impact, the meniscus is twisted by the knee bones, typically splitting parallel with the circumferentially oriented collagen fibers, resulting in a tear[20]. Moreover, meniscal injury is highly associated with impairment of movement, decreased joint stability and changes in knee joint mechanics and also a common source of pain[53].

Meniscal tears are common with young active people who suffer a sudden injury resulting in tearing[54]. Treatment of such tears depends on seriousness of the injury as smaller

tears can be treated with physiotherapy and rehabilitation of the knee[54]. Furthermore, in case of a serious tear, surgically sewing the meniscal tear or by partial meniscectomy, where part of the teared meniscal tissue is removed from the joint, is a common procedure[54]. However, partial meniscectomy can result in development of OA and thus it is not the best solution in all tear cases[55].

Degeneration of meniscus progresses with age even without a traumatic injury, occurring due to cartilage degeneration process, which is commonly associated with OA[56], [57]. In magnetic resonance imaging study, prevalence of meniscal tears in nontraumatic menisci have been found as high as over 50%[58]. Furthermore, prevalence and severity of nontraumatic meniscal tears have been shown to increase with age[59]. Degenerative meniscus is a source of pain and knee dysfunction with common symptoms including knee joint tenderness, locking of knee and aching[56]. Furthermore, a study has shown that patients with degenerative meniscal tears have similar movement impairing symptoms like reduced endurance and balance as with traumatic meniscus[57]. As with traumatic meniscus, the degenerative meniscus can lead to OA or *vice versa*[16].

In early OA, while meniscus seems to remain intact, fibrillations on the cartilaginous superficial layer can be observed together with disruptions, that slowly spread from inner border to all meniscal surfaces over time[44]. With the progress of the disease, more changes to the ECM of meniscus can be observed. Studies have found an increased content of water-binding PGs in degenerative and aged ECM of meniscus[35], [60]. As water content increases with the surge of PGs and collagen content decreases in relation to degeneration, the constituent balance in ECM changes dramatically and causes severe disorganization to the collagenous network[35]. Furthermore, abnormal cell clusters and hypertrophic cells have been found in the ECM that are associated with meniscal tears and surface degeneration[44]. In a study with canine, GAG content dropped dramatically after induction of OA, but returned to normal after several months and exceeded them after year and a half[60]. Together, these changes suggest that meniscal cartilage has some capacity to repair and regenerate itself[35].

As treatment of OA and meniscal tears are limited and without guaranteed recovery, early diagnosing and preventing the disease is crucial to preserve a healthy meniscus[61]. The golden standard in assessing knee OA in clinical world is the radiograph, which has limited possibilities in meniscus imaging[62]. Moreover, meniscus is a soft tissue and thus,

does not provide the required contrast to enable x-ray imaging *in vivo.* Another common method to *in vivo* imaging of meniscus is MRI[63], [64]. However, the resolution is not sensitive enough with either method to image the microstructural components of the meniscus and thus, an *ex vivo* approach to study meniscus contents is required[62]. In addition, following the progress of the disease and understanding the microstructural changes occurring inside the meniscus require more high-quality imaging modalities. Using *e.g.* μCT as imaging modality will benefit us with more reliable and sensitive imaging.

2.3 Micro-computed tomography

Plain radiography has been a common method to assess OA in the knee *e.g.* measuring joint space narrowing, [46], [65]. While joint space narrowing is associated with meniscal tears, plain radiography lacks information of the meniscal tissue. Thus, computed tomography (CT) has been used as a non-destructive, three-dimensional imaging method to image the knee joint[66]. The CT imaging is based on the attenuation of x-rays through the matter of the imaged object acquired from multiple viewing angles[67]. Modern CT devices have a large scale of resolutions available[68]. A standard CT device has a spatial resolution of approximately 0.5 millimetres and can image human sized objects[68].However, the resolution is not high enough for imaging of microscopic changes in the knee. Thus, for high resolution, microscopic imaging, a μCT device is preferred.

A standard μCT device achieves an isotropic voxel size of few micrometers[24]. On the contrary to the standard clinical CT device, the μCT device is smaller in size and imaged object size is up to 75 mm in diameter and 70 mm in height. The high resolution and small pixel size make μCT an excellent *ex vivo* imaging tool[25]. As of today, μCT devices are in a vital role in the analysis of 3D tissues including bone and cartilage[67].

2.3.1 Image formation in micro-computed tomography

A standard desktop μCT scanner has an x-ray source emitting x-rays that are collimated and filtered to a narrow energy spectrum and directed towards the imaged object[67]. The x-rays penetrate the material and are exponentially attenuated according to the material in its path. After, the attenuation is recorded by a 2D charge-coupled device array working as a detector. The object is then rotated around its long axis, while x-ray source and detector are in a fixed position and a new projection of the object is then acquired from a new angle. Moreover, this process is repeated until the object has been rotated 180 or 360 degrees around its long axis. A three-dimensional μCT image of the object can be reconstructed after a set of these 2D projections has been acquired[67]. Standard components of a working μCT device are seen in Figure 4.

In μCT imaging, the contrast between different tissues in an object are dependent on the tissues' ability to attenuate the x-rays as they penetrate them. The contrast is thus produced by tissue's physical contrast properties, density, thickness, and atomic number.

Attenuation coefficient is a quantified measure of how much the x-ray beam is attenuated by the material in a specific distance that it is penetrating through. Thus, differentiating two tissues with similar characteristics to each other requires the correct source energy combined with the right filter[67]. Furthermore, to compensate different gains in pixels to improve imaging quality further, dark and flat-field corrections are performed by acquiring images without the object between the source and detector before the imaging to create a uniform output[67], [69].

After acquisition of all needed projections, an image of the object is reconstructed from the information in the projections. Each projection of the object acquired from different direction contains an attenuation profile, that are commonly combined using reconstructive method called filtered back-projection. First, the attenuation profiles are low pass filtered to remove low frequency interference and then through convolution filter to reduce blurring or noise depending the image details. Moreover, the attenuation profiles are summed together to a matrix of the image, from which all the attenuation coefficients can be solved computationally. Filtered back-projection is prone to streaking and noise artifacts, which can be reduced with smaller rotation steps and frame averaging[70]. However, μCT imaging is always a compromise between balancing acquisition time and dataset size with image quality. Thus, the optimization and balancing between the scan acquisition times and image quality is crucial.

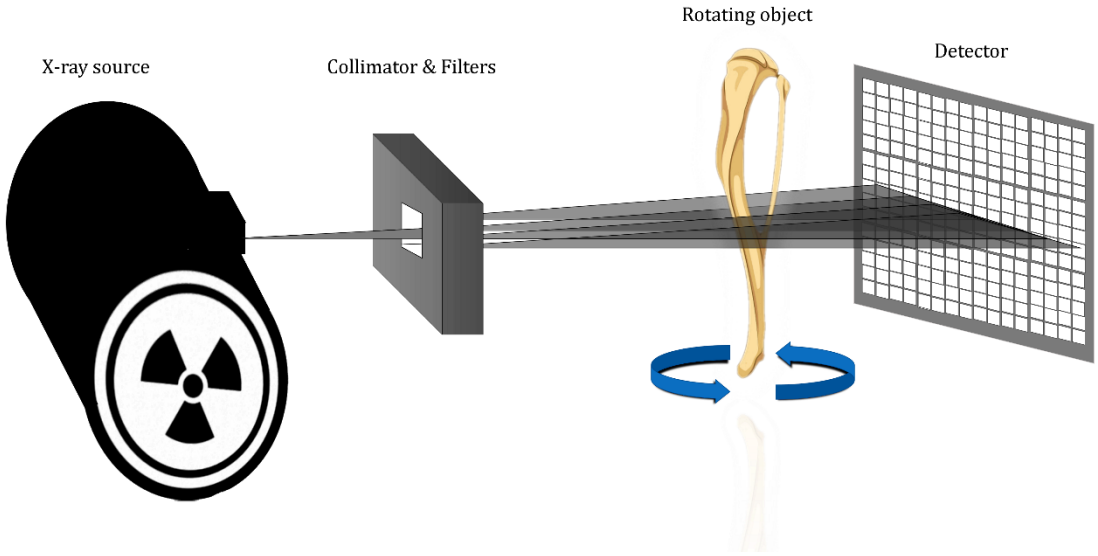

Figure 4. Standard components of a µCT desktop device. An x-ray tube emits x-rays which are collimated and filtered to a specific energy spectrum depending what structures are wanted to be observed. Filtered x-rays pass through the object and attenuated x-rays are then recorded by the CCD detector. Furthermore, the object rotates after and the process starts for the next projection.

2.3.2 Contrast enhanced micro-computed tomography

Although µCT imaging is predominantly used for imaging of hard tissues like bone due to its' high density and thickness which produces strong contrast in the image, imaging of soft tissues with µCT device is common nowadays with the help of contrast-enhancing methods[26]. In CEµCT, soft tissues' weak abilities to attenuate x-rays are enhanced by different methods, including drying *e.g.* with HMDS, in which the contrast arises from the tissue itself[29]. Another commonly used method is inducing contrast-agents that bind to specific compounds within the tissue to provide the required contrast in for µCT imaging[71]. However, while contrast agents provide apparent contrast between structures, the distribution of contrast agents in the tissue is affected by repulsion and attraction between different constituents in the tissue and contrast agent[72]. This may lead to inaccuracy while performing quantitative analysis and thus, using drying methods over contrast agents is preferred.

The aim of drying methods is to create contrast in soft tissue by dehydrating the biological tissue prior to imaging. Thus, the contrast emerges from the dried tissue and not from the contrast agent[73]. Although, drying of biological specimen causes shrinkage and requires extra effort to minimize it[73]. All sample drying methods including freeze drying

[74], critical-point drying[75] and HMDS-based drying [76] involve multiple steps to preserve the biological specimen in its original state after drying. The HMDS-based method requires the least expensive equipment while providing close to similar results with critical-point drying[76] .

HMDS-based, contrast-agent free μCT protocol has been used before to image chondrons in AC[72]. Furthermore, the protocol enabled imaging of the meniscus microstructure in 3D and the same protocol has already been used to measure microstructural orientation in AC[28], [29]. However, quantifying meniscus local microstructural orientation has not been done before in 3D.

2.4 Orientation analysis of structural components

The quantification of anisotropy, its direction and degree are a compelling research topic in multiple research fields including transportation, automotive and medical, mostly all dealing with different physical structures[77]–[79]. Furthermore, short fibre composites are nowadays used in many applications as reinforcer in the composite materials that require light weight, specific modulus, and high strength. Thus, the physical properties including stiffness, strength and impact behavior are mostly dependent of structural fibres in the materials structure[79]. Moreover, in the medical field, the interest of fibres arises from understanding changes in physical properties and behavior of biological tissue like fibrous proteins i.e. collagen[39]. Thus, understanding the state of the tissue, like its structural components' orientations, gains us more information on its possible physical properties.

2.4.1 Advancements in orientation analysis

Multiple different techniques to determine the fibre orientations in materials have been proposed during the last several decades[78], [80]. For instance, fibre orientations can be measured with global measurements when the orientations of each individual fibre are unknown. One of the earliest and most used global measurement techniques is mean-intercept length (MIL) which estimates the microstructure orientation and isotropy[81], [82]. MIL method tracks the number and distance of intersections between a group of parallel lines and interfaces[83]. MIL is a well-established method, but is boundary based and thus, it calculates the orientation of the interface rather that of the material[84].

Later, Odgaard et al. proposed a volume orientation (VO) method that was developed from MIL technique, by segmenting the 3D image into two phases of matrix and fibres[77]. VO works similar with MIL by calculating number of intercepts, but by lying a grid on the structure and determining the orientation of the longest intercept as the local volume orientation for each square in the grid[77].

Unlike MIL and VO methods working on global measurements, Mlekusch suggested an image analysis method based on individual measurements of fibres[85]. Moreover, the method measures the elliptic shape of fibre cross sections to evaluate the direction of fibre in the material[86], [87]. Ellipsometry is a nowadays a frequently used method to identify

fibre orientations in composite materials from 2D microscopy images[88]. However, problems arise from the loss of information from fibres parallel to cross-section plane and high amount of processed data required[88].

Unlike before, a new way of characterising the local fibre volume fraction and extracting the fibre orientations has been done from µCT images[89]. Evaluating fibre orientation distribution of composite materials was proposed by Straumit et al. using µCT images and structure tensors[90]. The method was certified for high resolution µCT images in comparison between Avizo's 3D fibre identification and 2D ellipsometry method[78].

All orientation analysing methods require high resolution scans, high computational resources, and analysis times from which the latter two scale substantially higher with larger volumes of interest (VOI) and integration windows. Here, VOI is the user defined volume within the 3D image used for the analyses and integration window defines the volume from which the structure tensors are calculated. Different resolutions in the µCT images show different orientation results for the object as with higher resolution you can observe more inhomogeneous distribution in structural orientations[78].

Overall, for resolutions that allow identification of individual fibres, the structure tensor analysis correlates well in results with other orientation characterization methods ellipsometry and Avizo. Furthermore, for resolutions that do not allow the former, structure tensor analysis generates results consistent with higher resolutions , unlike the two other orientation characterization methods[78].

2.4.2 Local orientation analysis

Structure tensor analysis is a method used in image processing, including analysis of µCT images[78], [80]. The technique to evaluate characteristics of the fibre orientation distribution using local structure tensors based on 3D µCT images was established by Straumit et al. in 2015[90].

For the structure tensor analysis, µCT image needs to be presented as gradients. Each voxel in the µCT images can be assigned a grey value and corresponding coordinates in the full µCT dataset. Thus, a µCT image can be represented as a 3D grey value function I(x, y, z). The principal direction and the degree of microstructural anisotropy is indicated

by this gradient and can be calculated using a structure tensor. Continuous structure tensor for three-dimensional space is defined as follows:

$$S(p) = \int_{W(p)} S'(r)\, dr \qquad S'(x,y,z) = \begin{bmatrix} \left(\frac{\partial I}{\partial x}\right)^2 & \frac{\partial I}{\partial x}\frac{\partial I}{\partial y} & \frac{\partial I}{\partial x}\frac{\partial I}{\partial z} \\ \frac{\partial I}{\partial x}\frac{\partial I}{\partial y} & \left(\frac{\partial I}{\partial y}\right)^2 & \frac{\partial I}{\partial y}\frac{\partial I}{\partial z} \\ \frac{\partial I}{\partial x}\frac{\partial I}{\partial z} & \frac{\partial I}{\partial y}\frac{\partial I}{\partial z} & \left(\frac{\partial I}{\partial z}\right)^2 \end{bmatrix} \quad (1),$$

where W(p) is the integration window, p is a vector defining the position of the integration window and r is a vector in the image with the components (x, y, z) in relation to the integration window.

Visualization of the process, integration window and structure tensor directions are seen in Figure 5. Actual size of the integration window is $(2w_r + 1)^3$ voxels, where w_r is a parameter for window size. Moreover, the value of window size should be approximately the diameter of the investigated fibres. The values of partial derivatives are calculated with a 5-point differentiation scheme which averages the greyscale values for the structure tensor within the defined integration window[90]. Furthermore, the eigenvalue decomposition for the structure tensor matrix is applied and presents three eigenvalues ($\lambda_1 \leq \lambda_2 \leq \lambda_3$), each with their respective eigenvectors (v_1, v_2, v_3) representing variability in the microstructure and its direction. The smallest eigenvalue λ_1 and its corresponding vector v_1 are chosen as they indicate the smallest variability in the microstructure and in which direction this smallest gradient variability is reached within the integration window. Furthermore, this direction is the principal direction of anisotropy and corresponds to the direction of local orientation. Moreover, the procedure to determine the principal direction is repeated for all voxels inside the VOI of the μCT dataset to determine the orientation for all structural components in the object..

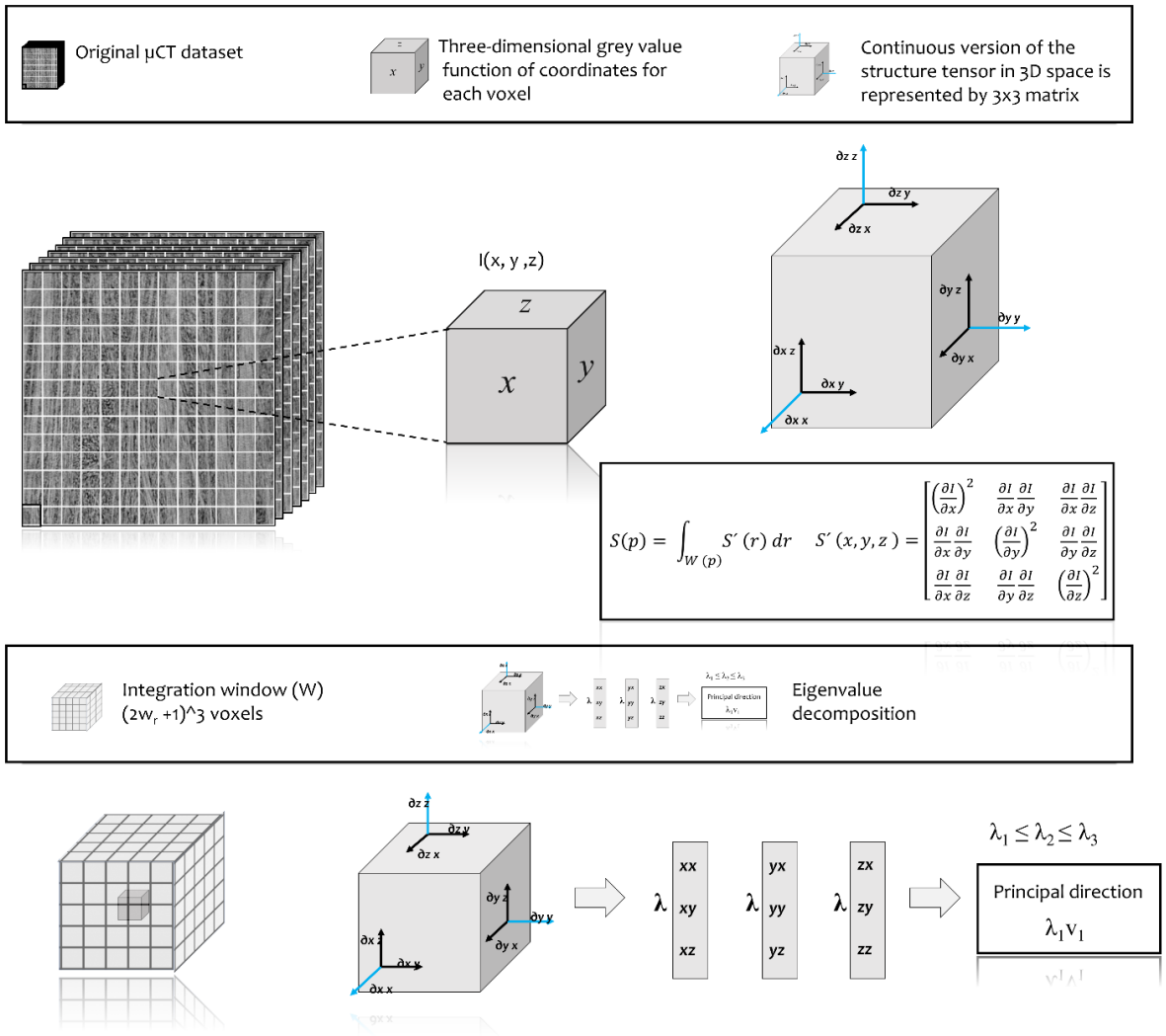

Figure 5. Micro-computed tomography dataset can be represented as three-dimensional grey value functions I (x, y, z) of coordinates in which the anisotropy of the microstructure is represented by the grey value gradient. Thus, structure tensor analysis allows the calculation of the principal direction $\lambda_1 v_1$ from this gradient. Continuous version of structure tensor in 3D space is represented as a 3x3 matrix. Integration window defines the volume in 3D space from which the gradients are calculated. Decomposition of the structure tensor gives three eigenvalues (λ_1, λ_2, λ_3) and corresponding eigenvectors (v_1, v_2, v_3). Minimum variability is reached in the smallest eigenvalue λ_1 and its corresponding vector v_1 indicating the direction of the minimum variability. Thus, this direction is the principal direction of anisotropy within the window and indicates the local fibre orientation.

3. OBJECTIVE OF THE STUDY

The objective of this study was to quantitatively analyze the microstructural organization of human meniscus posterior horn samples in 3D using HMDS-based μCT imaging. In addition, in this study we compare the local microstructural organization between end-stage medial compartment knee OA patients and healthy references.

4. CONCLUSIONS

In this study, we found that using our HMDS-based sample drying protocol with conventional desktop μCT imaging, we could quantitatively analyse the local microstructural organization of collagen network in the posterior horn of human meniscus in 3D.

Our results indicate major differences in the collagen organization between osteoarthritic and donor meniscus samples. We found higher disorganization of the collagen fibre network in the medial osteoarthritic menisci when compared to medial donor, lateral donor and lateral osteoarthritis menisci. Furthermore, this increased disorganization of collagen network in the medial osteoarthritic meniscus samples suggest a strong relationship between meniscus collagen disorganization and medial compartment knee OA. Furthermore, we found that lateral donor, medial donor, and lateral osteoarthritic samples had similar microstructural orientation distribution, which was expected, as the patients had end-stage OA diagnosed only in the medial compartment of meniscus.

5. REFERENCES

[1] M. Kloppenburg and F. Berenbaum, "Osteoarthritis year in review 2019: epidemiology and therapy," *Osteoarthritis and Cartilage*, vol. 28, no. 3. W.B. Saunders Ltd, pp. 242–248, Mar. 01, 2020, doi: 10.1016/j.joca.2020.01.002.

[2] J. Dekker, B. Boot, L. H. V. van der Woude, and J. W. J. Bijlsma, "Pain and disability in osteoarthritis: A review of biobehavioral mechanisms," *Journal of Behavioral Medicine*, vol. 15, no. 2. Kluwer Academic Publishers-Plenum Publishers, pp. 189–214, Apr. 1992, doi: 10.1007/BF00848325.

[3] D. T. Felson *et al.*, "Osteoarthritis: New insights - Part 1: The disease and its risk factors," in *Annals of Internal Medicine*, 2000, vol. 133, no. 8, pp. 635–646, doi: 10.7326/0003-4819-133-8-200010170-00016.

[4] D. J. Hunter, J. J. McDougall, and F. J. Keefe, "The Symptoms of Osteoarthritis and the Genesis of Pain," *Rheumatic Disease Clinics of North America*, vol. 34, no. 3. NIH Public Access, pp. 623–643, Aug. 2008, doi: 10.1016/j.rdc.2008.05.004.

[5] K. Huch, "Knee and ankle: Human joints with different susceptibility to osteoarthritis reveal different cartilage cellularity and matrix synthesis in vitro," *Arch. Orthop. Trauma Surg.*, vol. 121, no. 6, pp. 301–306, 2001, doi: 10.1007/s004020000225.

[6] A. S Anderson and R. F. Loeser, "Why is osteoarthritis an age-related disease?," *Best Practice and Research: Clinical Rheumatology*, vol. 24, no. 1. Baillière Tindall, pp. 15–26, Jan. 01, 2010, doi: 10.1016/j.berh.2009.08.006.

[7] V. B. Vad, D. R. Adin, and J. Solomon, "Knee osteoarthritis," *Critical Reviews in Physical and Rehabilitation Medicine*, vol. 16, no. 3. StatPearls Publishing, pp. 211–231, Jun. 29, 2004, doi: 10.1615/CritRevPhysRehabilMed.v16.i3.30.

[8] Fairbank and T. J., "Knee joint changes after meniscectomy.," *J. Bone Joint Surg. Am.*, vol. 30 B, no. 4, pp. 664–670, Nov. 1948, doi: 10.1302/0301-620x.30b4.664.

[9] A. M. Ahmed and D. L. Burke, "In-vitro measurement of static pressure distribution in synovial joints - Part I: Tibial surface of the knee," *J. Biomech. Eng.*, vol. 105, no. 3, pp. 216–225, Aug. 1983, doi: 10.1115/1.3138409.

[10] I. D. McDermott, S. D. Masouros, and A. A. Amis, "Biomechanics of the menisci of the knee," *Curr. Orthop.*, vol. 22, no. 3, pp. 193–201, Jun. 2008, doi: 10.1016/j.cuor.2008.04.005.

[11] C. A. Haraden, J. L. Huebner, M. F. Hsueh, Y. J. Li, and V. B. Kraus, "Synovial fluid biomarkers associated with osteoarthritis severity reflect macrophage and neutrophil related inflammation," *Arthritis Res. Ther.*, vol. 21, no. 1, Jun. 2019, doi: 10.1186/s13075-019-1923-x.

[12] I. D. McDermott and A. A. Amis, “The consequences of meniscectomy,” *Journal of Bone and Joint Surgery - Series B*, vol. 88, no. 12. The British Editorial Society of Bone and Joint Surgery, pp. 1549–1556, Dec. 01, 2006, doi: 10.1302/0301-620X.88B12.18140.

[13] B. L. Keith Markolf, J. S. Mensch, and H. C. Amstutz, “The Journal of Bone and Joint Surgery Stiffness and Laxity of the Knee-The Contributions of the Supporting Structures A QUANTITATIVE in Vitro STUDY*t.”

[14] N. G. Shrive, J. J. O’Connor, and J. W. Goodfellow, “Load-bearing in the knee joint,” *Clin. Orthop. Relat. Res.*, vol. NO.131, no. 131, pp. 279–287, Mar. 1978, doi: 10.1097/00003086-197803000-00046.

[15] A. J. S. Fox, F. Wanivenhaus, A. J. Burge, R. F. Warren, and S. A. Rodeo, “The human meniscus: A review of anatomy, function, injury, and advances in treatment,” *Clinical Anatomy*, vol. 28, no. 2. John Wiley and Sons Inc., pp. 269–287, Mar. 01, 2015, doi: 10.1002/ca.22456.

[16] M. Englund, A. Guermazi, and S. L. Lohmander, “The Role of the Meniscus in Knee Osteoarthritis: a Cause or Consequence?,” *Radiologic Clinics of North America*, vol. 47, no. 4. pp. 703–712, Jul. 2009, doi: 10.1016/j.rcl.2009.03.003.

[17] L. D. Bennett and J. C. Buckland-Wright, “Meniscal and articular cartilage changes in knee osteoarthritis: A cross-sectional double-contrast macroradiograpahic study,” *Rheumatology*, vol. 41, no. 8, pp. 917–923, Aug. 2002, doi: 10.1093/rheumatology/41.8.917.

[18] J. Christoforakis, R. Pradhan, J. Sanchez-Ballester, N. Hunt, and R. K. Strachan, “Is there an association between articular cartilage changes and degenerative meniscus tears?,” *Arthrosc. - J. Arthrosc. Relat. Surg.*, vol. 21, no. 11, pp. 1366–1369, Nov. 2005, doi: 10.1016/j.arthro.2005.08.031.

[19] W. P. Chan *et al.*, “Osteoarthritis of the knee: Comparison of radiography, CT, and MR imaging to assess extent and severity,” *Am. J. Roentgenol.*, vol. 157, no. 4, pp. 799–806, Jan. 1991, doi: 10.2214/ajr.157.4.1892040.

[20] M. Englund, F. W. Roemer, D. Hayashi, M. D. Crema, and A. Guermazi, “Meniscus pathology, osteoarthritis and the treatment controversy,” *Nat. Rev. Rheumatol.*, vol. 8, no. 7, pp. 412–419, Jul. 2012, doi: 10.1038/nrrheum.2012.69.

[21] V. P. Mantripragada, W. Gao, N. S. Piuzzi, C. D. Hoemann, G. F. Muschler, and R. J. Midura, “Comparative Assessment of Primary Osteoarthritis Progression Using Conventional Histopathology, Polarized Light Microscopy, and Immunohistochemistry,” *Cartilage*, 2020, doi: 10.1177/1947603520938455.

[22] E. K. Danso, J. M. T. Oinas, S. Saarakkala, S. Mikkonen, J. Töyräs, and R. K. Korhonen, “Structure-function relationships of human meniscus,” *J. Mech. Behav. Biomed. Mater.*, vol. 67, pp. 51–60, Mar. 2017, doi: 10.1016/j.jmbbm.2016.12.002.

[23] D. Mittelstaedt, Y. Xia, A. Shmelyov, N. Casciani, and A. Bidthanapally, “Quantitative determination of morphological and territorial structures of articular

cartilage from both perpendicular and parallel sections by polarized light microscopy," *Connect. Tissue Res.*, vol. 52, no. 6, pp. 512–522, Dec. 2011, doi: 10.3109/03008207.2011.595521.

[24] M. L. Bouxsein, S. K. Boyd, B. A. Christiansen, R. E. Guldberg, K. J. Jepsen, and R. Müller, "Guidelines for assessment of bone microstructure in rodents using micro-computed tomography," *Journal of Bone and Mineral Research*, vol. 25, no. 7. John Wiley & Sons, Ltd, pp. 1468–1486, Jul. 01, 2010, doi: 10.1002/jbmr.141.

[25] J. S. Rhodes, T. R. P. Ford, J. A. Lynch, P. J. Liepins, and R. V. Curtis, "Micro-computed tomography: a new tool for experimental endodontology," *Int. Endod. J.*, vol. 32, no. 3, pp. 165–170, May 1999, doi: 10.1046/j.1365-2591.1999.00204.x.

[26] H. Lusic and M. W. Grinstaff, "X-ray-computed tomography contrast agents," *Chemical Reviews*, vol. 113, no. 3. American Chemical Society, pp. 1641–1666, Mar. 13, 2013, doi: 10.1021/cr200358s.

[27] B. A. Lakin, D. J. Grasso, R. C. Stewart, J. D. Freedman, B. D. Snyder, and M. W. Grinstaff, "Contrast enhanced CT attenuation correlates with the GAG content of bovine meniscus," *J. Orthop. Res.*, vol. 31, no. 11, pp. 1765–1771, Nov. 2013, doi: 10.1002/jor.22421.

[28] L. Rieppo *et al.*, "Determination of Extracellular Matrix Orientation of Articular Cartilage in 3D Using Micro-Computed Tomography," *Osteoarthr. Cartil.*, vol. 25, p. S254, Apr. 2017, doi: 10.1016/j.joca.2017.02.428.

[29] I. Kestilä *et al.*, "Three-dimensional microstructure of human meniscus posterior horn in health and osteoarthritis," *Osteoarthr. Cartil.*, vol. 27, no. 12, pp. 1790–1799, Dec. 2019, doi: 10.1016/j.joca.2019.07.003.

[30] K. Messner and J. Gao, "The menisci of the knee joint. Anatomical and functional characteristics, and a rationale for clinical treatment," *J. Anat.*, vol. 193, no. 2, pp. 161–178, Aug. 1998, doi: 10.1046/j.1469-7580.1998.19320161.x.

[31] H. Aagaard and R. Verdonk, "Function of the normal meniscus and consequences of meniscal resection," *Scand. J. Med. Sci. Sports*, vol. 9, no. 3, pp. 134–140, Jan. 2007, doi: 10.1111/j.1600-0838.1999.tb00443.x.

[32] P. S. Walker and M. J. Erkman, "The role of the menisci in force transmission across the knee," *Clin. Orthop. Relat. Res.*, no. 109, p. 184—192, 1975, doi: 10.1097/00003086-197506000-00027.

[33] A. S. Voloshin and J. Wosk, "Shock absorption of meniscectomized and painful knees: A comparative in vivo study," *J. Biomed. Eng.*, vol. 5, no. 2, pp. 157–161, 1983, doi: 10.1016/0141-5425(83)90036-5.

[34] V. Mow and R. Huiskes, *Basic orthopaedic biomechanics & mechano-biology*, 3rd ed. Philadelphia: Lippincott Williams & Wilkins, 2005.

[35] J. Herwig, E. Egner, and E. Buddecke, "Chemical changes of human knee joint menisci in various stages of degeneration," *Ann. Rheum. Dis.*, vol. 43, no. 4, pp. 635–640, 1984, doi: 10.1136/ard.43.4.635.

[36] C. A. McDevitt and R. J. Webber, “The ultrastructure and biochemistry of meniscal cartilage,” in *Clinical Orthopaedics and Related Research*, no. 252, 1990, pp. 8–18.

[37] F. N. Ghadially, J. M. Lalonde, and J. H. Wedge, “Ultrastructure of normal and torn menisci of the human knee joint.,” *J. Anat.*, vol. 136, no. Pt 4, pp. 773–91, Jun. 1983, Accessed: Aug. 17, 2020. [Online]. Available: http://www.ncbi.nlm.nih.gov/pubmed/6688412.

[38] M. E. Adams, C. A. McDevitt, A. Ho, and H. Muir, “Isolation and characterization of high-buoyant-density proteoglycans from semilunar menisci.,” *J. Bone Joint Surg. Am.*, vol. 68, no. 1, pp. 55–64, Jan. 1986, Accessed: Aug. 17, 2020. [Online]. Available: http://www.ncbi.nlm.nih.gov/pubmed/3753604.

[39] A. J. S. Fox, A. Bedi, and S. A. Rodeo, “The Basic Science of Human Knee Menisci: Structure, Composition, and Function,” *Sports Health*, vol. 4, no. 4, pp. 340–351, Jul. 2012, doi: 10.1177/1941738111429419.

[40] U. G. Longo, M. Loppini, G. Romeo, N. Maffulli, and V. Denaro, “Histological scoring systems for tissue-engineered, ex vivo and degenerative meniscus,” *Knee Surgery, Sport. Traumatol. Arthrosc.*, vol. 21, no. 7, pp. 1569–1576, Jul. 2013, doi: 10.1007/s00167-012-2142-z.

[41] D. Johnson, T. Swenson, … C. H.-O. S. for S. M. 19th, and U. 1993, “Arthroscopic meniscal transplantation: Anatomic and technical considerations,” Sun Valley, 1993.

[42] R. M. Aspden, Y. E. Yarker, and D. W. Hukins, “Collagen orientations in the meniscus of the knee joint.,” *J. Anat.*, vol. 140 (Pt 3, pp. 371–80, May 1985, Accessed: Jan. 21, 2020. [Online]. Available: http://www.ncbi.nlm.nih.gov/pubmed/4066476.

[43] W. Petersen and B. Tillmann, “Collagenous fibril texture of the human knee joint menisci,” *Anat. Embryol. (Berl).*, vol. 197, no. 4, pp. 317–324, 1998, doi: 10.1007/s004290050141.

[44] C. Pauli *et al.*, “Macroscopic And Histopathologic Analysis Of Human Knee Menisci In Aging And Osteoarthritis,” *Osteoarthr. Cartil.*, vol. 19, no. 9, pp. 1132–1141, Sep. 2011, doi: 10.1016/j.joca.2011.05.008.

[45] T. Bhattacharyya *et al.*, “The clinical importance of meniscal tears demonstrated by magnetic resonance imaging in osteoarthritis of the knee,” *J. Bone Jt. Surg. - Ser. A*, vol. 85, no. 1, pp. 4–9, Jan. 2003, doi: 10.2106/00004623-200301000-00002.

[46] S. K. Das and A. Farooqi, “Osteoarthritis,” *Best Practice and Research: Clinical Rheumatology*, vol. 22, no. 4. pp. 657–675, Aug. 2008, doi: 10.1016/j.berh.2008.07.002.

[47] A. Mobasheri, A. C. Bay-Jensen, W. E. van Spil, J. Larkin, and M. C. Levesque, “Osteoarthritis Year in Review 2016: biomarkers (biochemical markers),” *Osteoarthritis and Cartilage*, vol. 25, no. 2. W.B. Saunders Ltd, pp. 199–208, Feb.

01, 2017, doi: 10.1016/j.joca.2016.12.016.

[48] M. Cross *et al.*, "The global burden of hip and knee osteoarthritis: Estimates from the Global Burden of Disease 2010 study," *Ann. Rheum. Dis.*, vol. 73, no. 7, pp. 1323–1330, 2014, doi: 10.1136/annrheumdis-2013-204763.

[49] R. C. Lawrence *et al.*, "Estimates of the prevalence of arthritis and selected musculoskeletal disorders in the United States," *Arthritis Rheum.*, vol. 41, no. 5, pp. 778–799, May 1998, doi: 10.1002/1529-0131(199805)41:5<778::AID-ART4>3.0.CO;2-V.

[50] F. S. Hanna *et al.*, "Factors affecting patella cartilage and bone in middle-aged women," *Arthritis Rheum.*, vol. 57, no. 2, pp. 272–278, Mar. 2007, doi: 10.1002/art.22535.

[51] M. Englund, E. M. Roos, and L. S. Lohmander, "Impact of type of meniscal tear on radiographic and symptomatic knee osteoarthritis: A sixteen-year followup of meniscectomy with matched controls," *Arthritis Rheum.*, vol. 48, no. 8, pp. 2178–2187, Aug. 2003, doi: 10.1002/art.11088.

[52] B. D. Browner, J. B. Jupiter, A. M. Levine, and P. G. Trafton, *Skeletal trauma: basic science, management and reconstruction*, 3rd ed. Philadelphia, PA: Saunders, 2003.

[53] Y. Katsuragawa *et al.*, "Changes of human menisci in osteoarthritic knee joints," *Osteoarthr. Cartil.*, vol. 18, no. 9, pp. 1133–1143, Sep. 2010, doi: 10.1016/j.joca.2010.05.017.

[54] O. Saarelma, "Polvivamma, kierukkavamma, ristisidevamma," *Duodecim Kustannus OY*, 2020. https://www.terveyskirjasto.fi/terveyskirjasto/tk.koti?p_teos=&p_artikkeli=dlk00772 (accessed Dec. 10, 2020).

[55] B. T. Feeley and B. C. Lau, "Biomechanics and Clinical Outcomes of Partial Meniscectomy," *J. Am. Acad. Orthop. Surg.*, vol. 26, no. 24, pp. 853–863, Dec. 2018, doi: 10.5435/JAAOS-D-17-00256.

[56] A. K. Lange *et al.*, "Degenerative meniscus tears and mobility impairment in women with knee osteoarthritis," *Osteoarthr. Cartil.*, vol. 15, no. 6, pp. 701–708, Jun. 2007, doi: 10.1016/j.joca.2006.11.004.

[57] R. Howell, N. S. Kumar, N. Patel, and J. Tom, "Degenerative meniscus: Pathogenesis, diagnosis, and treatment options," *World J. Orthop.*, vol. 5, no. 5, pp. 597–602, 2014, doi: 10.5312/wjo.v5.i5.597.

[58] A. Guermazi, S. Zaim, B. Taouli, Y. Miaux, C. G. Peterfy, and H. K. Genant, "MR findings in knee osteoarthritis," *Eur. Radiol.*, vol. 13, no. 6, pp. 1370–1386, Jun. 2003, doi: 10.1007/s00330-002-1554-4.

[59] S. Fukuta, K. Masaki, and F. Korai, "Prevalence of abnormal findings in magnetic resonance images of asymptomatic knees," *J. Orthop. Sci.*, vol. 7, no. 3, pp. 287–291, May 2002, doi: 10.1007/s007760200049.

[60] M. E. Adams, M. E. J. Billingham, and H. Muir, “The glycosaminoglycans in menisci in experimental and natural osteoarthritis,” *Arthritis Rheum.*, vol. 26, no. 1, pp. 69–76, Jan. 1983, doi: 10.1002/art.1780260111.

[61] E. Rath and J. C. Richmond, “The menisci: Basic science and advances in treatment,” *British Journal of Sports Medicine*, vol. 34, no. 4. pp. 252–257, 2000, doi: 10.1136/bjsm.34.4.252.

[62] A. J. Teichtahl, A. E. Wluka, M. L. Davies-Tuck, and F. M. Cicuttini, “Imaging of knee osteoarthritis,” *Best Practice and Research: Clinical Rheumatology*, vol. 22, no. 6. Baillière Tindall, pp. 1061–1074, Dec. 01, 2008, doi: 10.1016/j.berh.2008.09.004.

[63] M. Englund *et al.*, “Incidental meniscal findings on knee MRI in middle-aged and elderly persons,” *N. Engl. J. Med.*, vol. 359, no. 11, pp. 1108–1115, Sep. 2008, doi: 10.1056/NEJMoa0800777.

[64] T. Georgiev *et al.*, “Cartilage oligomeric protein, matrix metalloproteinase-3, and Coll2-1 as serum biomarkers in knee osteoarthritis: a cross-sectional study,” *Rheumatol. Int.*, vol. 38, no. 5, pp. 821–830, May 2018, doi: 10.1007/s00296-017-3887-y.

[65] N. Maffulli, U. G. Longo, S. Campi, and V. Denaro, “Meniscal tears,” in *The 5-Minute Sports Medicine Consult: Second Edition*, vol. 1, Wolters Kluwer Health Adis (ESP), 2012, pp. 45–54.

[66] A. P. Toms, L. M. White, T. J. Marshall, and S. T. Donell, “Imaging the post-operative meniscus,” *Eur. J. Radiol.*, vol. 54, no. 2, pp. 189–198, May 2005, doi: 10.1016/j.ejrad.2005.01.024.

[67] M. Stauber and R. Müller, “Micro-computed tomography: A method for the non-destructive evaluation of the three-dimensional structure of biological specimens,” *Methods Mol. Biol.*, vol. 455, pp. 273–292, 2008, doi: 10.1007/978-1-59745-104-8_19.

[68] E. Lin and A. Alessio, “What are the basic concepts of temporal, contrast, and spatial resolution in cardiac CT?,” *J. Cardiovasc. Comput. Tomogr.*, vol. 3, no. 6, pp. 403–408, Nov. 2009, doi: 10.1016/j.jcct.2009.07.003.

[69] V. Patel, R. N. Chityala, K. R. Hoffmann, C. N. Ionita, D. R. Bednarek, and S. Rudin, “Self-calibration of a cone-beam micro-CT system,” *Med. Phys.*, vol. 36, no. 1, pp. 48–58, 2009, doi: 10.1118/1.3026615.

[70] R. Blanco Sequeiros, S. Koskinen, H. Aronen, N. Lundbom, R. Vanninen, and O. Tervonen, *Kliininen radiologia*, 1. painos. Duodecim, 2017.

[71] S. S. Karhula *et al.*, “Effects of articular cartilage constituents on phosphotungstic acid enhanced micro-computed tomography,” *PLoS One*, vol. 12, no. 1, Jan. 2017, doi: 10.1371/journal.pone.0171075.

[72] I. Kestilä *et al.*, “In vitro method for 3D morphometry of human articular cartilage chondrons based on micro-computed tomography,” *Osteoarthr. Cartil.*, vol. 26,

no. 8, pp. 1118–1126, Aug. 2018, doi: 10.1016/j.joca.2018.05.012.

[73] M. L. Reed and G. K. Fedder, “2. Photolithographic microfabrication,” in *Handbook of Sensors and Actuators*, vol. 6, Elsevier, 1998, pp. 13–61.

[74] F. Yu *et al.*, “Mechanism research on a bioactive resveratrol– PLA–gelatin porous nano-scaffold in promoting the repair of cartilage defect,” *Int. J. Nanomedicine*, vol. 13, pp. 7845–7858, 2018, doi: 10.2147/IJN.S181855.

[75] M. Kaliva, G. S. Armatas, and M. Vamvakaki, “Microporous polystyrene particles for selective carbon dioxide capture,” *Langmuir*, vol. 28, no. 5, pp. 2690–2695, Feb. 2012, doi: 10.1021/la204991n.

[76] J. L. Nation, “A new method using hexamethyldisilazane for preparation of soft insect tissues for scanning electron microscopy,” *Biotech. Histochem.*, vol. 58, no. 6, pp. 347–351, 1983, doi: 10.3109/10520298309066811.

[77] A. Odgaard, E. B. Jensen, and H. J. G. Gundersen, “Estimation of structural anisotropy based on volume orientation. A new concept,” *J. Microsc.*, vol. 157, no. 2, pp. 149–162, Feb. 1990, doi: 10.1111/j.1365-2818.1990.tb02955.x.

[78] R. Karamov, L. M. Martulli, M. Kerschbaum, I. Sergeichev, Y. Swolfs, and S. V. Lomov, “Micro-CT based structure tensor analysis of fibre orientation in random fibre composites versus high-fidelity fibre identification methods,” *Compos. Struct.*, vol. 235, p. 111818, Mar. 2020, doi: 10.1016/j.compstruct.2019.111818.

[79] K. Friedrich and A. A. Almajid, “Manufacturing Aspects of Advanced Polymer Composites for Automotive Applications,” *Springer*, 2012, doi: 10.1007/s10443-012-9258-7.

[80] P. Pinter, S. Dietrich, B. Bertram, L. Kehrer, P. Elsner, and K. A. Weidenmann, “Comparison and error estimation of 3D fibre orientation analysis of computed tomography image data for fibre reinforced composites,” *NDT E Int.*, vol. 95, pp. 26–35, Apr. 2018, doi: 10.1016/j.ndteint.2018.01.001.

[81] W. J. Whitehouse, “The quantitative morphology of anisotropic trabecular bone,” *J. Microsc.*, vol. 101, no. 2, pp. 153–168, Jul. 1974, doi: 10.1111/j.1365-2818.1974.tb03878.x.

[82] R. A. Ketcham and T. M. Ryan, “Quantification and visualization of anisotropy in trabecular bone,” *J. Microsc.*, vol. 213, no. 2, pp. 158–171, Feb. 2004, doi: 10.1111/j.1365-2818.2004.01277.x.

[83] R. Moreno, M. Borga, and Ö. Smedby, “Generalizing the mean intercept length tensor for gray-level images,” *Med. Phys.*, vol. 39, no. 7, pp. 4599–4612, 2012, doi: 10.1118/1.4730502.

[84] F. De Pascalis and M. Nacucchi, “Volume orientation: a practical solution to analyse the orientation of fibres in composite materials,” *J. Microsc.*, vol. 276, no. 1, pp. 27–38, Oct. 2019, doi: 10.1111/jmi.12832.

[85] B. Mlekusch, “Fibre orientation in short-fibre-reinforced thermoplastics II.

Quantitative measurements by image analysis," *Compos. Sci. Technol.*, vol. 59, no. 4, pp. 547–560, Mar. 1999, doi: 10.1016/S0266-3538(98)00101-8.

[86] K. S. Lee, S. W. Lee, J. R. Youn, T. J. Kang, and K. Chung, "Confocal microscopy measurement of the fiber orientation in short fiber reinforced plastics," *Fibers Polym.*, vol. 2, no. 1, pp. 41–50, Mar. 2001, doi: 10.1007/bf02875227.

[87] C. Eberhardt, A. Clarke, M. Vincent, T. Giroud, and S. Flouret, "Fibre-orientation measurements in short-glass-fibre compsites - II: A quantitative error estimate of the 2D image analysis technique," *Compos. Sci. Technol.*, vol. 61, no. 13, pp. 1961–1974, Oct. 2001, doi: 10.1016/S0266-3538(01)00106-3.

[88] R. Blanc, C. Germain, J. P. Da Costa, P. Baylou, and M. Cataldi, "Fiber orientation measurements in composite materials," *Compos. Part A Appl. Sci. Manuf.*, vol. 37, no. 2, pp. 197–206, Feb. 2006, doi: 10.1016/j.compositesa.2005.04.021.

[89] G. Requena, G. Fiedler, B. Seiser, P. Degischer, M. Di Michiel, and T. Buslaps, "3D-Quantification of the distribution of continuous fibres in unidirectionally reinforced composites," *Compos. Part A Appl. Sci. Manuf.*, vol. 40, no. 2, pp. 152–163, Feb. 2009, doi: 10.1016/j.compositesa.2008.10.014.

[90] I. Straumit, S. V. Lomov, and M. Wevers, "Quantification of the internal structure and automatic generation of voxel models of textile composites from X-ray computed tomography data," *Compos. Part A Appl. Sci. Manuf.*, vol. 69, pp. 150–158, 2015, doi: 10.1016/j.compositesa.2014.11.016.

6. APPENDICES

Appendix 1:

Karjalainen V-P, Kestilä I, Finnilä MA, et al. Quantitative three-dimensional collagen orientation analysis of human meniscus posterior horn in health and osteoarthritis using micro-computed tomography. Accepted as a full-length original research article in Osteoarthritis and Cartilage. Pre-proof of the article published online February 13, 2021. doi:10.1016/j.joca.2021.01.009